

# Capacitive Micromachined Ultrasonic Transducers (CMUTs) for Photoacoustic Imaging

Srikant Vaithilingam<sup>a,\*</sup>, Ira O. Wygant<sup>a</sup>, Paulina S. Kuo<sup>a</sup>, Xuefeng Zhuang<sup>a</sup>, Ömer Oralkan<sup>a</sup>, Peter D. Olcott<sup>b</sup> and Butrus T. Khuri-Yakub<sup>a</sup>

<sup>a</sup>Edward L. Ginzton Laboratory, Stanford University, Stanford, CA 94305-4088, USA;

<sup>b</sup>Department of Radiology, Stanford University, Stanford, CA 94305-5344, USA

## ABSTRACT

In photoacoustic (optoacoustic) medical imaging, short laser pulses irradiate absorbing structures found in tissue, such as blood vessels, causing brief thermal expansions that in turn generate ultrasound waves. These ultrasound waves which correspond to the optical absorption distribution were imaged using a two-dimensional array of capacitive micromachined ultrasonic transducers (CMUTs). Advantages of CMUT technology for photoacoustic imaging include the ease of integration with electronics, ability to fabricate large two-dimensional arrays, arrays with arbitrary geometries, wide-bandwidth arrays and high-frequency arrays. In this study, a phantom consisting of three 0.86-mm inner diameter polyethylene tubes inside a tissue mimicking material was imaged using a 16 x 16 element CMUT array. The center tube was filled with India-ink to provide optical contrast. Traditional pulse-echo data as well as photoacoustic image data were taken. 2D cross-sectional slices and 3D volume rendered images are shown. Simple array tiling was attempted, whereby a 48 x 48 element array was simulated, to illustrate the advantages of larger arrays. Finally, the sensitivity of the photoacoustics setup to the concentration of ink in the tube was also explored. For the sensitivity experiment a different phantom consisting of only one 1.14-mm inner diameter polyethylene tube inside a tissue mimicking material was used. The concentration of the ink inside the tube was varied and images were taken.

**Keywords:** CMUT, high-frequency, laser, ultrasound, photoacoustic, optoacoustic, integrated electronics, imaging

## 1. INTRODUCTION

There has been extensive interest in developing new techniques for noninvasive medical imaging. Photoacoustic imaging (PAI), also called optoacoustic imaging, is a promising medical imaging technology because it combines the contrast information of optical imaging with the spatial resolution of acoustic imaging. Potential clinical applications for PAI include cancer detection, functional imaging and molecular imaging.<sup>1</sup> In PAI, the target tissue is illuminated with short laser pulses that causes brief heating of absorbing structures like blood vessels. The induced temperature increase generates acoustic pressure waves due to the thermoelastic effect. These pressure waves propagate to the surface of the tissue where they can be detected with ultrasound transducers. Those regions that are more optically absorbent than others will generate a stronger ultrasound signal. Using the ultrasound data, an image of the optical absorption properties of the material can be constructed. For medical imaging, photoacoustics is interesting because materials in the body have different optical absorption coefficients, which is a wavelength dependent tissue property. Thus, oxygenated or deoxygenated hemoglobin (Fig. 1), water or melanin etc, can be distinguished based on their absorbed spectrum.<sup>2</sup> Laser pulse widths of around 10 ns and wavelengths between 600 nm and 1000 nm are typically used for photoacoustic imaging.<sup>1,3-5</sup> The wavelength is chosen to provide sufficient penetration and good optical contrast between the materials being imaged. The pulse length must be brief enough such that the volume expansions are short and efficiently generate ultrasound. Photoacoustic imaging has been extensively studied. Notable results have been published for the imaging of humans and small animals.<sup>1,3-6</sup>

---

Further author information: (Send correspondence to Srikant Vaithilingam)

Srikant Vaithilingam:- E-mail: srikantv@stanford.edu, Telephone: 1 650 723 0297; <http://piezo.stanford.edu>

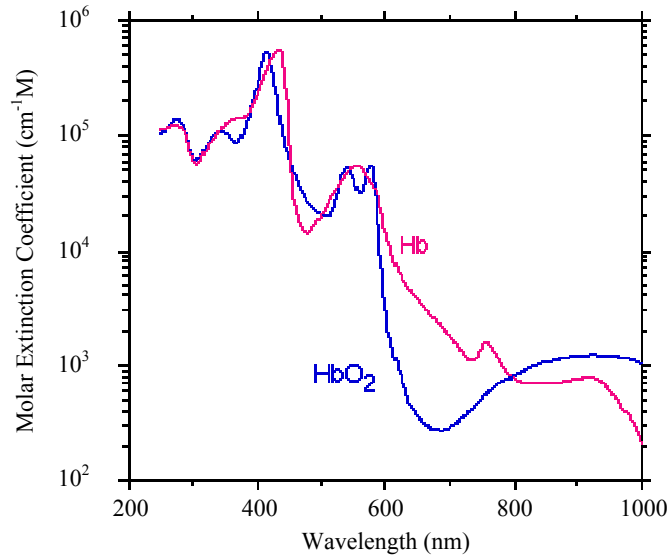


**Figure 1.** Optical absorption spectrum of hemoglobin. The spectrum shows the oxygen dependent absorption at different wavelengths. The molar extinction coefficient is proportional to the optical absorption coefficient (spectrum from <http://omlc.ogi.edu/>).

Unlike suitable excitation lasers, which are commercially available, the perfect transducer, a key part of PAI, remains to be developed. The ideal acoustic transducer should provide high axial and lateral resolution, strong sensitivity, wide bandwidth, should be transparent to the exciting laser pulse and should ideally acquire a whole three-dimensional (3D) image at one shot, without scanning, at fast frame rates.<sup>7</sup> These requirements partially contradict each other (i.e. resolution and sensitivity) or are limited by current technology (3D acquisition and transparency to laser pulse). In this work we propose using a capacitive micromachined ultrasonic transducer (CMUT) array to overcome some of these limitations. Previous photoacoustic imaging work has typically relied on a single mechanically scanned focused piezoelectric transducer for detection of the laser-generated ultrasound. Using a CMUT array in place of a mechanically scanned element has a number of advantages. 3D images can be acquired in one shot using large, two-dimensional arrays which can be reliably fabricated using CMUT technology. Arbitrary CMUT array geometries such as the ring array have been demonstrated.<sup>8</sup> A ring array has the practical benefit that the laser light can come through the hole in the center of the array. CMUTs typically have wider bandwidths than comparable piezoelectric transducers. This could be especially significant given the broadband nature of the laser-generated ultrasound. Since CMUTs can be integrated with electronics, this reduces the parasitics in the electronics and improves noise performance, thus improving image quality.

## 2. EXPERIMENTAL SETUP

### 2.1. Single Array

A diagram illustrating the experimental setup is shown in Fig. 2a. For these experiments, the phantom to be imaged is suspended in an oil tank of size 5 cm x 5 cm x 3 cm. Vegetable oil is used to couple ultrasound between the array and phantom. Vegetable oil is also used because it is nonconducting and thus the array and electronics do not need to be insulated. The phantom consists of three 0.86-mm inner diameter (1.27-mm outer diameter) polyethylene tubes passing through a 2 cm x 2 cm x 3 cm block of tissue mimicking material (ATS Laboratories, Bridgeport, CT). The center tube is filled with India-ink to provide optical contrast for the photoacoustic imaging. The CMUT array is located at the bottom of the tank. The phantom is illuminated from the side of the tank by a Q-switched Nd:YAG laser. Ideally the laser should uniformly illuminate the material being imaged. Thus the laser beam is de-focused to a  $1/e^2$  diameter of approximately 6 mm. A ground glass diffuser in front of the tank further diffuses the laser light. The laser used has a 1.064  $\mu\text{m}$  wavelength and 12-ns

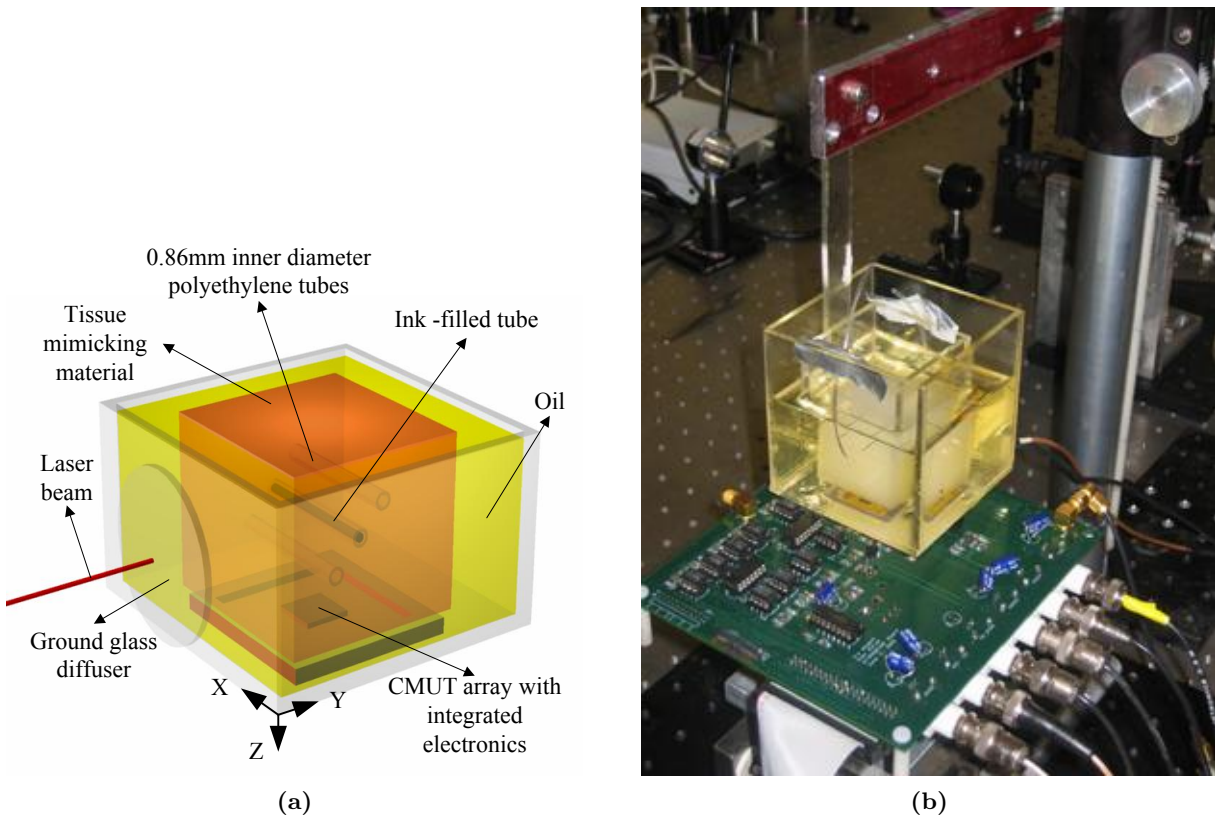


**Figure 2.** Experimental Setup: (a) Vessel-like photoacoustic imaging phantom. Three 0.86-mm inner diameter tubes are inside a block of tissue mimicking material. The center tube is filled with ink to provide optical contrast. The phantom is illuminated by a laser from the side. (b) Photograph of the phantom and tank. The transducer array is located at the bottom of the tank.

FWHM pulse duration. The energy of each laser pulse is 2.3 mJ. The laser was fired at a rate of 10 Hz. A photograph of the phantom and tank is shown in Fig. 2b.

## 2.2. Array Tiling

CMUT technology allows the fabrication of large two-dimensional arrays. The advantages of larger arrays include the ability to image larger targets with an improved signal to noise ratio. Larger arrays also result in improved lateral resolution due to a larger aperture size. To simulate this effect, array tiling was performed. In our experiment the CMUT array was placed on an X-Y translational stage. After one data set was acquired, the array was translated 4 mm (length of the array) along the x-direction and another data set was acquired. Further data sets were obtained by also translating 4 mm along the y-direction. In all, 9 data-sets were acquired in the positions shown in Fig. 3. Hence, the intention is that array tiling will result in an image that will be equivalent to an image taken with an array of size 48 x 48 elements.

## 3. CMUT AND INTEGRATED ELECTRONICS

The transducer array has 256 elements (16 x 16 elements). Each element is  $250\ \mu\text{m} \times 250\ \mu\text{m}$ . Thus, the entire array size is 4 mm x 4 mm. The transducers have a center frequency of 5 MHz. The CMUT array was fabricated using surface micromachining with membranes made of silicon nitride. A few of the key CMUT device parameters are shown in Table. 1. A picture of the packaged device is shown in Fig. 4a. The CMUT array and electronics are shown in Fig. 4b. A more thorough description of the design and fabrication of the CMUT array has been reported elsewhere.<sup>9</sup> A description of the CMUT array and integrated electronics has

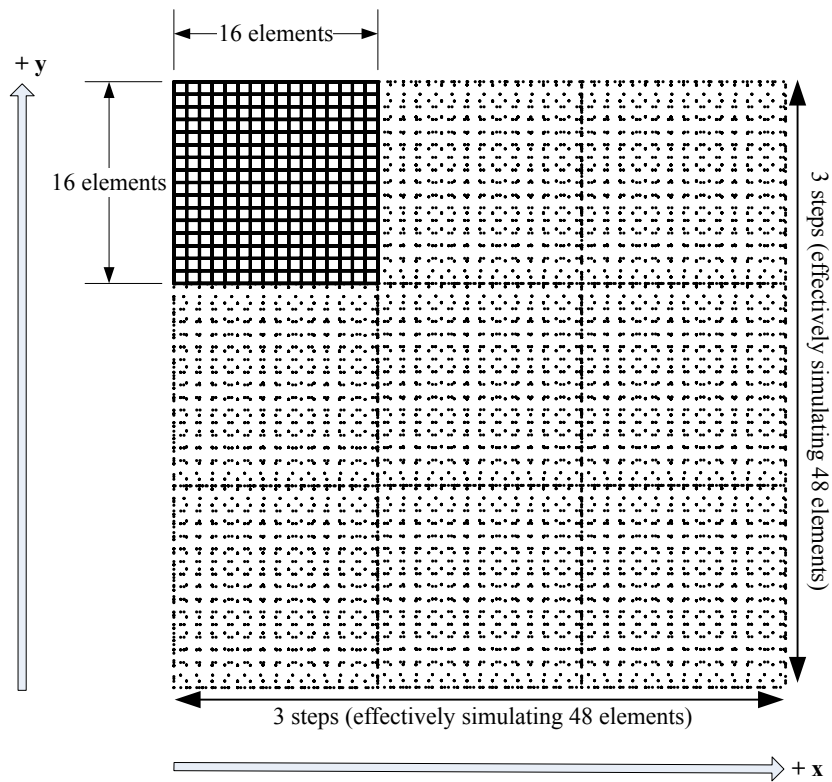


**Figure 3.** Tiling: The CMUT Array is translated along the x-direction to simulate a larger array of size 48 x 48 elements.

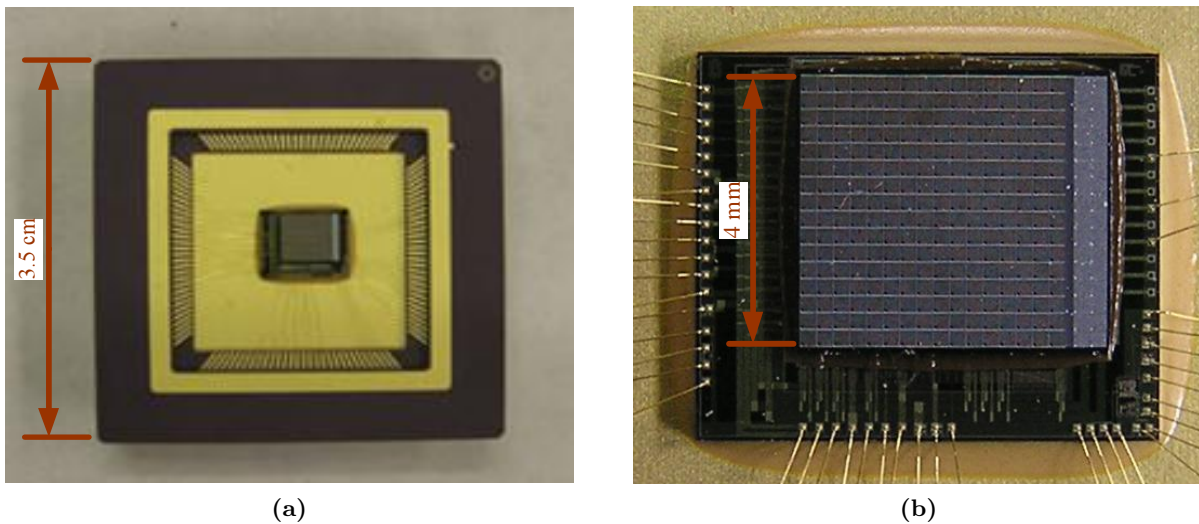


**Figure 4.** Electronics: (a) Package containing the transducer array and electronics. (b) CMUT array flip-chip bonded to an integrated circuit that comprises the front-end circuitry.

**Table 1.** CMUT Device Parameters

Cell diameter, $\mu\text{m}$	36
Element pitch, $\mu\text{m}$	250
Number of cells per element	24
Membrane thickness, $\mu\text{m}$	0.6
Cavity thickness, $\mu\text{m}$	0.1
Insulating layer thickness, $\mu\text{m}$	0.15
Silicon substrate thickness, $\mu\text{m}$	400
Flip-chip bond pad diameter, $\mu\text{m}$	50
Through-wafer interconnect diameter, $\mu\text{m}$	20

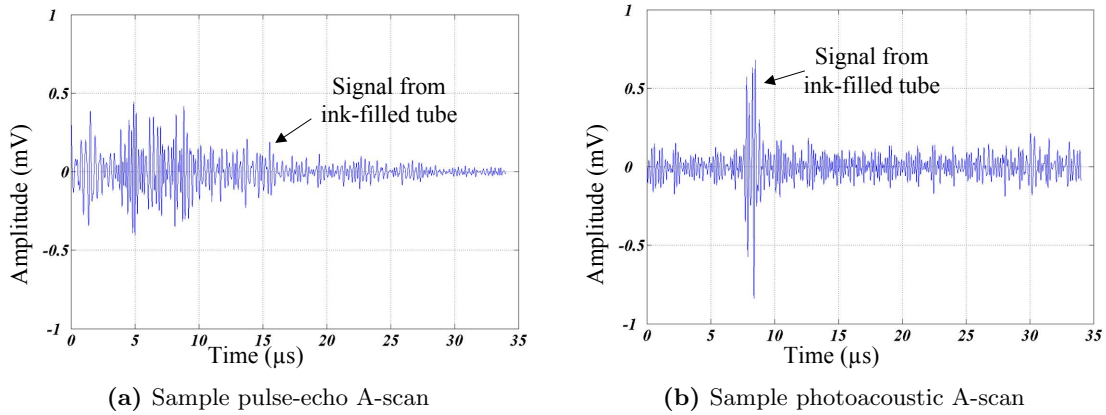


**Figure 5.** Sample A-scans: (a) Data acquired from a single element. The reflections from the 3 tubes can be identified. (b) The signal from the ink-filled tube can be seen clearly. The time at which the signal from the ink-filled tube is acquired is different for (a) and (b) since the photoacoustic data is acquired only in receive mode.

also been previously reported.<sup>10</sup> The transducer array is flip-chip bonded to a custom-designed integrated circuit (IC) that comprises the front-end circuitry. The result is that each element is connected to its own amplifier via a 400  $\mu\text{m}$  long through-wafer via. Integrating the electronics in this manner mitigates the effect of parasitic cable capacitance and simplifies connecting the transducer array to an external system. The IC allows for the selection of a single element at a time. Thus, 256 pulses are required to acquire a single image with no averaging. For a propagation limited system, this allows a maximum achievable frame rate of 100 frames/sec for imaging a 3 cm volume in oil.

## 4. RESULTS

### 4.1. Sample A-scans

Example pulse-echo and photoacoustic data acquisitions are shown in Fig. 5. The signal from the ink-filled tube can be identified in both figures. The individual element acquisitions are bandpass filtered and then used for image reconstruction. As is evident, the ink-filled tube gives a very strong signal in the photoacoustic A-scan.

### 4.2. Single Array

Conventional pulse-echo imaging data and photoacoustic imaging data were acquired for the phantom. Photoacoustic data was acquired by recording an element's output after the laser excitation. The pulse-echo data was averaged 64 times to improve the signal-to-noise ratio. The photoacoustic data was averaged 4 times. These images are shown in Fig. 6. In Fig. 6c the walls of the middle tube can be seen clearly. In Fig. 6e all three tubes can be seen, with the top two being more clear. Both the photoacoustic image and pulse-echo image are

constructed using a standard delay and sum image reconstruction algorithm. A 3D image of the photoacoustic image overlaid on the pulse-echo image is shown in Fig. 7. The ink is shown in red color over the middle tube.

### 4.3. Array Tiling

Consecutive slices in the XZ plane are shown for pulse-echo and photoacoustic data in Fig. 8 and Fig. 9 respectively. This is to illustrate the increased clarity resulting from array tiling. The length of the tube in Fig. 8 is longer than the single array image in Fig. 6c. In Fig. 8 it can clearly be seen that the tube curves upwards. The volume rendered images are shown in Fig. 10. A volume rendered image of the photoacoustic tiled image overlaid on the pulse-echo tiled image is shown in Fig. 11. The ink is shown as a reddish glow over the middle tube.

## 5. ONGOING WORK

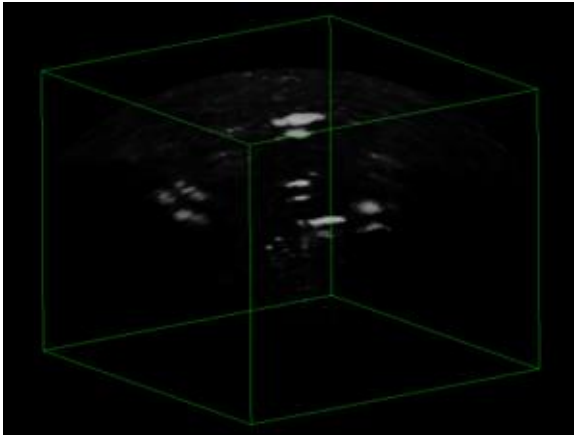
The sensitivity of the CMUT with this laser is under investigation. The experimental setup used is similar to the one described in section 2, with the only difference being the phantom. The phantom consists of one 1.14-mm inner diameter (1.57-mm outer diameter) polyethylene tube passing through a 4 cm x 4 cm x 4 cm block of tissue mimicking material (ATS Laboratories, Bridgeport, CT). The phantom is positioned such that the tube is 2 cm above the CMUT array and filled with India-ink to provide optical contrast for the photoacoustic imaging. The concentration of the India ink is varied in powers of 1/2 and images are taken. A simple integration of the pixel values in a volume surrounding the ink-tube is performed on each image. These values are then normalized. Initial results from this experiment are summarized in the graph shown in Fig. 12. Sample images taken at various concentrations of ink are shown in Fig. 13.

## 6. CONCLUSION

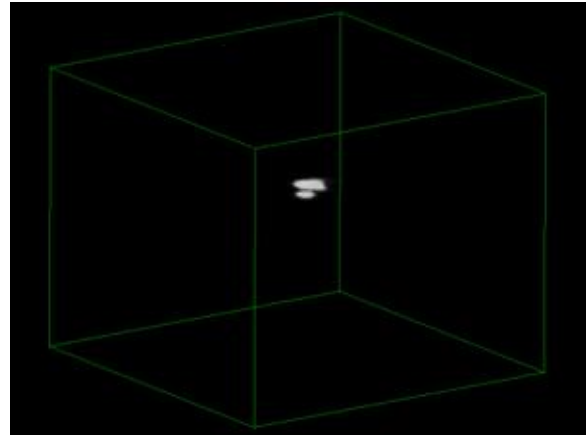
Photoacoustic images obtained with a CMUT transducer array and integrated electronics are presented. These results demonstrate some of the advantages of CMUT technology for photoacoustic imaging. A transducer array such as the one used in this work has clear acquisition time advantages over a mechanically scanned system. By increasing the laser repetition rate, real-time images could be obtained with the system described here. Image resolution could be improved by using a larger aperture size. An attempt to illustrate this was made by array tiling. CMUT arrays as large as 128 x 128 elements have been fabricated.<sup>11</sup> The use of such large CMUT arrays for photoacoustic imaging would provide both outstanding image quality yet allow for fast acquisition times.

## ACKNOWLEDGMENTS

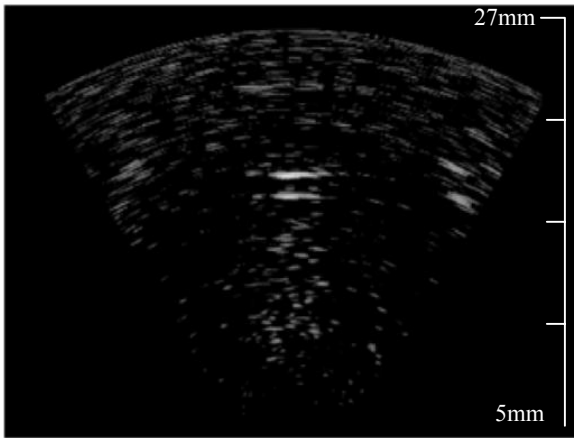
Funding was provided by the National Institute of Health. The authors would like to thank National Semiconductor for the fabrication of the integrated circuits. Bill Broach and the members of the portable power group at National Semiconductor provided valuable circuit and process discussions. Shay Keren from the Molecular Imaging Program, Stanford University provided valuable assistance in conducting the experiments. Ed Binkley of Promex Industries, Santa Clara, CA provided packaging and flip-chip bonding support. Srikant Vaithilingam is supported by a P. Michael Farmwald Stanford Graduate Fellowship. Xuefeng Zhuang is supported by a Weiland Family Stanford Graduate Fellowship.



(a) 3D volume-rendered pulse-echo image



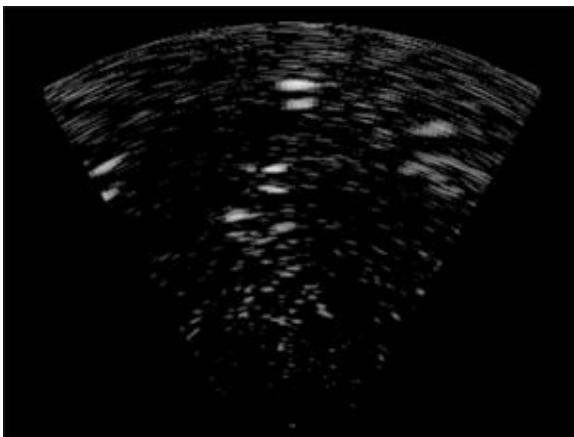
(b) 3D volume-rendered photoacoustic image



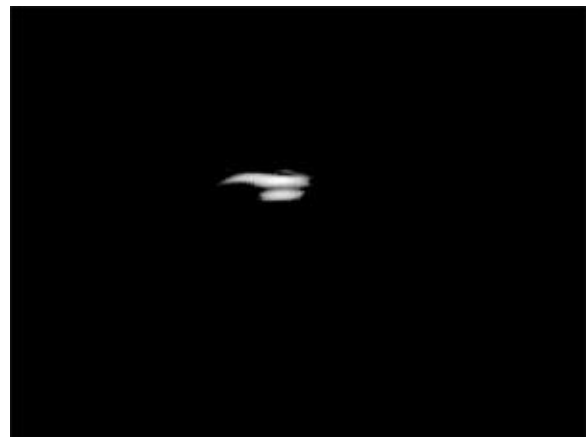
(c) pulse-echo: XZ slice, 20 dB dynamic range



(d) photoacoustic: XZ slice, 15 dB dynamic range



(e) pulse-echo: YZ slice, 20 dB dynamic range



(f) photoacoustic: YZ slice, 15 dB dynamic range

**Figure 6.** Ultrasound Images: (a) Volume rendered pulse-echo image of the phantom. (b) Volume rendered photoacoustic image of the phantom. (c) and (e) are the XZ and YZ slices taken from the 3D volume pulse-echo image with 20 dB dynamic range. (d) and (f) are the XZ and YZ slices taken from the 3D volume photoacoustic image with 15 dB dynamic range.

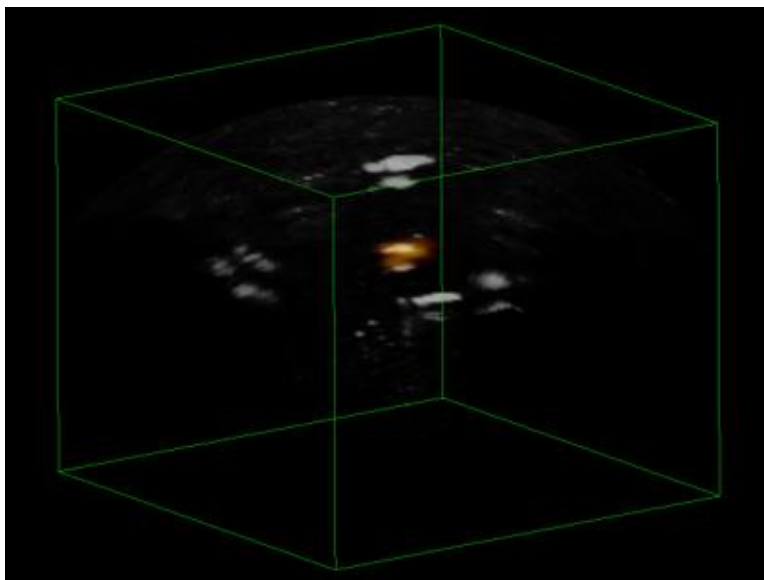


**Figure 7.** 3D volume rendered fusion of pulse-echo and photoacoustic images taken from a single array. Photoacoustic data is shown in red.

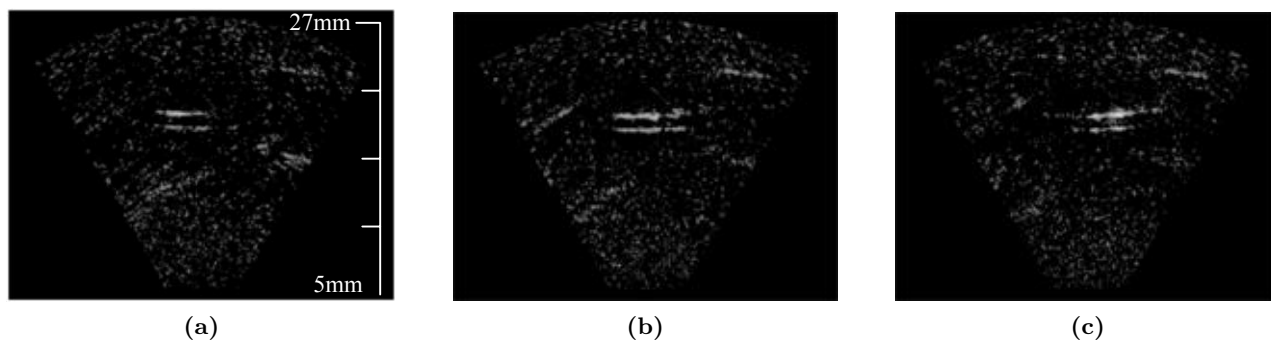


**Figure 8.** Consecutive pulse-echo images in the XZ plane taken from a 3D pulse-echo volume image with 25 dB dynamic range. Shows the tube curving upwards.

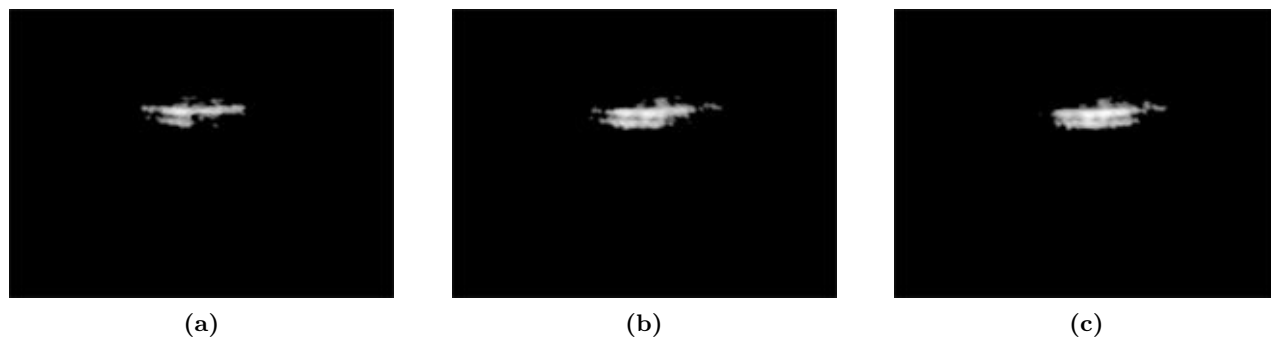
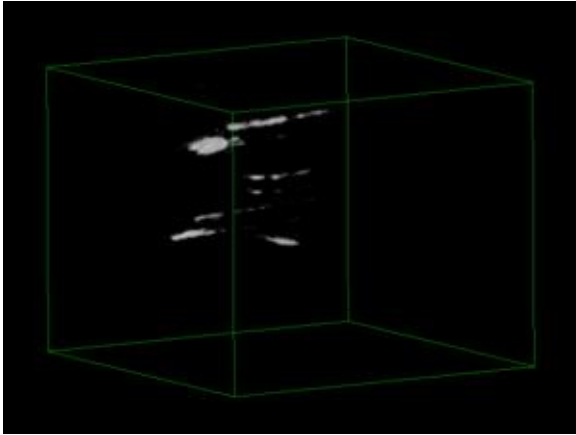
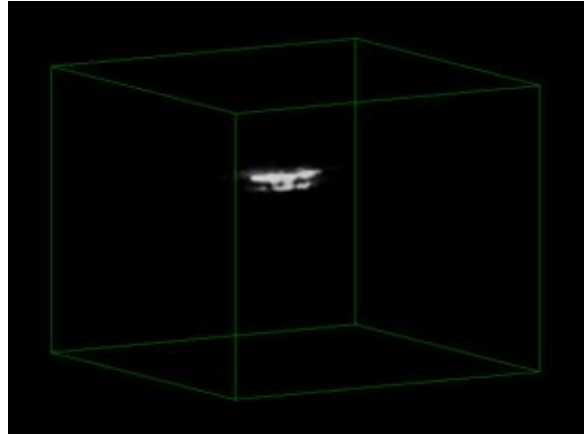


**Figure 9.** Consecutive photoacoustic images in the XZ plane taken from a 3D photoacoustic volume image with 20 dB dynamic range.



(a) 3D volume-rendered pulse-echo image taken with array tiling (simulating 48 x 48 element array)



(b) 3D volume-rendered photoacoustic image taken with array tiling (simulating 48 x 48 element array)

**Figure 10.** Tiled ultrasound Images: (a) Tiled volume rendered pulse-echo images of the phantom shown. Note how the walls of the tube are clearly seen.(b) Tiled volume-rendered photoacoustic image.

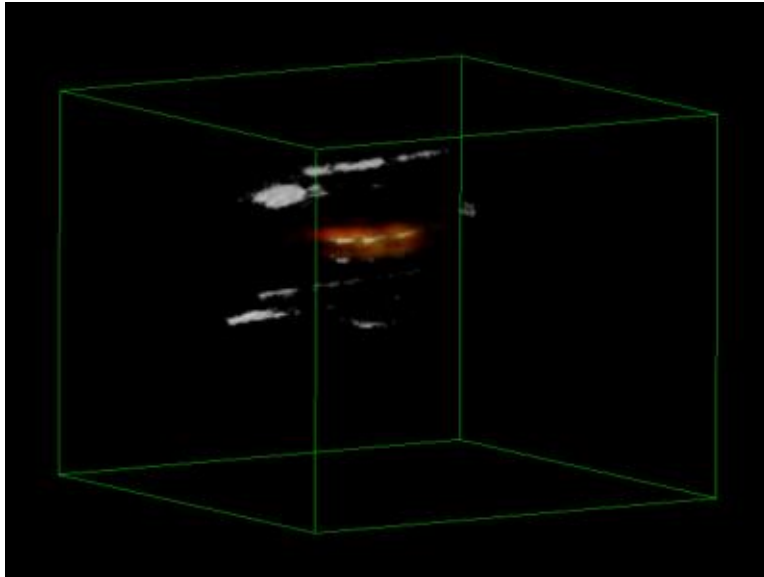


**Figure 11.** Tiled 3D volume-rendered fusion of pulse-echo and photoacoustic images. Photoacoustic data seen in red color.

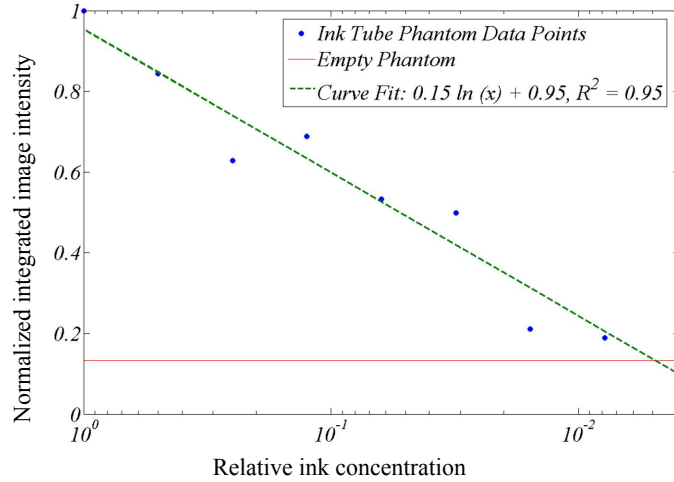
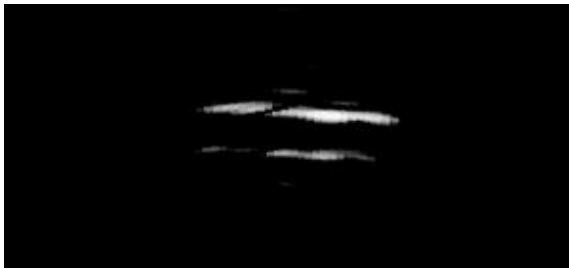
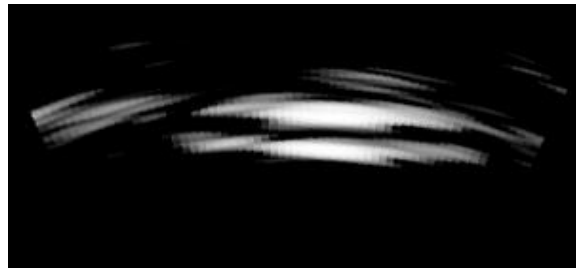


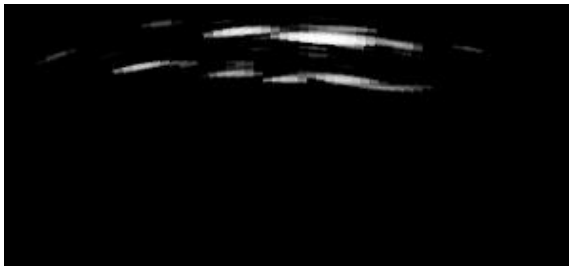
**Figure 12.** Graph of normalized integrated image intensity against ink concentration.



(a) Pulse-echo image of undiluted India-ink.



(b) Photoacoustic image of undiluted India-ink.



(c) Pulse-echo image of India-ink diluted by  $2^2$ .



(d) Photoacoustic image of India-ink diluted by  $2^2$ .



(e) Pulse-echo image of India-ink diluted by  $2^5$ .



(f) Photoacoustic image of India-ink diluted by  $2^5$ .

**Figure 13.** Sample images at various ink concentrations. Images have a 20 dB dynamic range relative to the undiluted ink.

## REFERENCES

1. L. Wang, "Ultrasound-mediated biophotonic imaging: a review of acousto-optical tomography and photo-acoustic tomography," *Journal of Disease Markers* **19**, pp. 123–138, 2004.
2. J. J. Niederhauser, M. Jaeger, and M. Frenz, "Comparison of laser-induced and classical ultrasound," in *Biomedical Optoacoustics IV*, A. A. Oraevsky, ed., *Proc. SPIE* **4960**, pp. 118–123, 2003.
3. C. G. A. Hoelen and F. F. M. de Mul, "Image reconstruction for photo-acoustic scanning of tissue structures," *Applied Optics* **39**, pp. 5872–5883, 2000.
4. C. G. A. Hoelen, F. F. M. de Mul, R. Pongers, and A. Dekker, "Three-dimensional photo-acoustic imaging of blood vessels in tissue," *Optics Letters* **23**, pp. 648–650, 1999.
5. R. O. K. Esenaliev, A. A. Karabutov, and A. A. Oraevsky, "Sensitivity of laser opto-acoustic imaging in detection of small deeply embedded tumors," *IEEE J Sel Top Quantum* **5**, pp. 981–988, 1999.
6. J. Niederhauser, M. Jaeger, R. Lemor, P. Weber, and M. Frenz, "Combined ultrasound and optoacoustic system for real-time high-contrast vascular imaging *in Vivo*," *IEEE Transactions on Medical Imaging* **24**(4), pp. 436–440, 2004.
7. J. J. Niederhauser, M. Jaeger, and M. Frenz, "Real-time three-dimensional optoacoustic imaging using an acoustic lens system," *Applied Physics Letters* **85**(5), pp. 846–848, 2004.
8. D. T. Yeh, O. Oralkan, I. O. Wygant, M. O'Donnell, and B. T. Khuri-Yakub, "3-d ultrasound imaging using forward viewing cmut ring arrays for intravascular and intracardiac applications," *IEEE International Ultrasonics Symposium*, (Rotterdam, The Netherlands), Sept 2005.
9. X. Zhuang, I. O. Wygant, D. T. Yeh, A. Nikoozadeh, O. Oralkan, A. S. Ergun, C.-H. Cheng, Y. Huang, G. G. Yaralioglu, and B. T. Khuri-Yakub, "Two-dimensional capacitive micromachined ultrasonic transducer (cmut) arrays for a miniature integrated volumetric ultrasonic imaging system," in *Medical Imaging: Ultrasonic Imaging and Signal Processing*, W. F. Walker and S. Y. Emelianov, eds., *Proc. SPIE* **5750**, pp. 37–46, 2005.
10. I. O. Wygant, D. T. Yeh, X. Zhuang, A. Nikoozadeh, O. Oralkan, A. S. Ergun, M. Karaman, and B. T. Khuri-Yakub, "A miniature real-time volumetric ultrasound imaging system," in *Medical Imaging: Ultrasonic Imaging and Signal Processing*, W. F. Walker and S. Y. Emelianov, eds., *Proc. SPIE* **5750**, pp. 26–36, 2005.
11. O. Oralkan, A. S. Ergun, C. H. Cheng, J. A. Johnson, M. Karaman, T. H. Lee, and B. T. Khuri-Yakub, "Volumetric ultrasound imaging using 2-d cmut arrays," *IEEE Trans. Ultrason., Ferroelect., Freq. Contr* **50**(11), pp. 1581–1594, 2003.